Oncogene (2011) 30, 4740–4749

www.nature.com/onc

ORIGINAL ARTICLE

Opposite modifying effects of HR and NHEJ deficiency on cancer risk in *Ptc1* heterozygous mouse cerebellum

M Tanori[1], E Pasquali[2], S Leonardi[1], P Giardullo[2], V Di Majo[1], G Taccioli[3], J Essers[4,7], R Kanaar[4], LH Mullenders[5], MJ Atkinson[6], M Mancuso[1], A Saran[1] and S Pazzaglia[1]

[1]*Laboratory of Radiation Biology and Biomedicine, Agenzia Nazionale per le Nuove Tecnologie, l'Energia e lo Sviluppo Economico Sostenibile (ENEA) CR-Casaccia, Rome, Italy;* [2]*Department of Radiation Physics, Università degli Studi Guglielmo Marconi, Rome, Italy;* [3]*Departments of Molecular and Cellular Biology, Goldman School of Dental Medicine, Boston University, Boston, MA, USA;* [4]*Department of Cell Biology and Genetics, Cancer Genomics Center, and Department of Radiation Oncology, Erasmus Medical Center, Rotterdam, The Netherlands;* [5]*Department of Toxicogenetics, Leiden University Medical Centre, Leiden, The Netherlands;* [6]*Institute of Pathology, Helmholtz Zentrum München-German Research Center for Environment and Health, Neuherberg, Germany and* [7]*Department of Vascular Surgery, Erasmus Medical Center, Rotterdam, The Netherlands*

Heterozygous *Patched1* (*Ptc1*$^{+/-}$) mice are prone to medulloblastoma (MB), and exposure of newborn mice to ionizing radiation dramatically increases the frequency and shortens the latency of MB. In *Ptc1*$^{+/-}$ mice, MB is characterized by loss of the normal remaining *Ptc1* allele, suggesting that genome rearrangements may be key events in MB development. Recent evidence indicates that brain tumors may be linked to defects in DNA-damage repair processes, as various combinations of targeted deletions in genes controlling cell-cycle checkpoints, apoptosis and DNA repair result in MB in mice. Non-homologous end joining (NHEJ) and homologous recombination (HR) contribute to genome stability, and deficiencies in either pathway predispose to genome rearrangements. To test the role of defective HR or NHEJ in tumorigenesis, control and irradiated *Ptc1*$^{+/-}$ mice with two, one or no functional *Rad54* or DNA–protein kinase catalytic subunit (*DNA–PKcs*) alleles were monitored for MB development. We also examined the effect of *Rad54* or *DNA–PKcs* deletion on the processing of endogenous and radiation-induced double-strand breaks (DSBs) in neural precursors of the developing cerebellum, the cells of origin of MB. We found that, although HR and NHEJ collaborate in protecting cells from DNA damage and apoptosis, they have opposite roles in MB tumorigenesis. In fact, although *Rad54* deficiency increased both spontaneous and radiation-induced MB development, *DNA–PKcs* disruption suppressed MB tumorigenesis. Together, our data provide the first evidence that *Rad54*-mediated HR *in vivo* is important for suppressing tumorigenesis by maintaining genomic stability.
Oncogene (2011) **30,** 4740–4749; doi:10.1038/onc.2011.178; published online 23 May 2011

Keywords: radiation; *Rad54*; *DNA–PKcs*; LOH; medulloblastoma

Correspondence: Dr A Saran or Dr S Pazzaglia, Laboratory of Radiation Biology and Biomedicine, Agenzia Nazionale per le Nuove Tecnologie, l'Energia e lo Sviluppo Economico Sostenibile (ENEA) CR-Casaccia, 00123 Rome, Italy.
E-mail: anna.saran@enea.it or simonetta.pazzaglia@enea.it
Received 24 February 2011; revised 5 April 2011; accepted 6 April 2011; published online 23 May 2011

Introduction

Somatic loss of heterozygosity (LOH) is a common genetic mechanism leading to complete loss of function of tumor suppressor genes in both sporadic and familial cancers (Tischfield and Shao, 2003). The critical tumor suppressor p53, for instance, is mutated in more than half of all inherited and spontaneously arising human cancers, often through LOH. Loss or inactivation of both alleles is also a prerequisite for tumor growth in individuals with heritable cancer syndromes in which each cell in the body carries a heterozygous mutation of the critical tumor suppressor gene. As an example, *PATCHED1* (*PTC1*) represents a human tumor suppressor gene and PTCH1 functions as a sonic hedgehog receptor protein and negative regulator of the pathway. Germline heterozygous mutations of *Ptc1* responsible for the Gorlin syndrome predispose to developmental defects and several types of cancer. Inactivating mutations of the remaining *Ptc1* allele occur via LOH in many of these tumors (Levanat *et al*., 1996). The *Ptc1* heterozygous knockout mice (*Ptc1*$^{+/-}$) represent the mouse model for Gorlin syndrome, and increased susceptibility to spontaneous and radiation-induced tumor development is a feature of these mice. In this model, *Ptc1* heterozygous mutation leads to the development of preneoplastic/early neoplastic stages in the skin and cerebellum of asymptomatic mice. Somatic loss of the remaining intact copy of *Ptc1* is the causal event in the transition from the preneoplastic to full-blown tumor stages in basal cell carcinoma and medulloblastoma (MB) (Pazzaglia *et al*., 2002; Mancuso *et al*., 2004; Pazzaglia *et al*., 2006a).

Although the molecular mechanisms for LOH are poorly defined, double-strand breaks (DSBs) have been suggested as initiating lesions for these events (Moynahan and Jasin, 1997). DSBs are frequently generated endogenously during normal cellular processes, such as DNA replication, or exogenously by exposure to a variety of genotoxic agents, such as ionizing radiation. A role for DSBs in *Ptc1* LOH is supported by the dramatic increase in MB tumorigenesis

in *Ptc1*$^{+/-}$ mice after exposure to ionizing radiation (Pazzaglia *et al*., 2002).

At least two distinct mechanisms contribute to DNA DSB repair; homologous recombination (HR), which takes advantage of either the homologous chromosome or the sister chromatid to join the broken DNA ends (Li and Heyer, 2008), and non-homologous end joining (NHEJ), which directly joins the DSB with little or no sequence homology between the broken ends (Cahill *et al*., 2006). Both pathways, through deletional or recombinational mechanisms, have the potential to cause genetic rearrangements, thus playing a critical role in maintaining genomic stability and preventing cancer. Major players in HR are the MRN (Mre11–RAD50–NBS1/XRS2) complex, RAD51, RAD54 and the RAD51 paralogs. In NHEJ, after end modification by the DNA–protein kinase complex (DNA–PK catalytic subunit (DNA–PKcs), Ku70, Ku80), ligation of the DNA ends is catalyzed by DNA ligase IV in conjunction with its binding partner XRCC4. Genetic evidence supports the concept of HR and NHEJ as distinct yet competing DSB repair pathways. The balance between them differs widely among species, among different cell types of a single species, and during different cell-cycle phases of a single cell type. The question as to whether HR or NHEJ will be used by the cell to repair a particular break is still an active area of investigation.

Knocking out genes in mice has facilitated the identification of DNA repair genes critical for oncogenesis. In the cerebellum, inactivation of *Ligase IV*, *Xrcc2*, *Brca2* and PARP-1 together with targeted deletion of p53 causes rapid MB development (Lee and McKinnon, 2002; Tong *et al*., 2003; Frappart *et al*., 2007, 2009). In keeping with this, we have recently shown that inactivation of PARP-1 strongly sensitizes the cells of the skin and cerebellum to radiation-induced oncogenesis in *Ptc1*$^{+/-}$ mice (Tanori *et al*., 2008). In the present study, to evaluate the relative contribution of HR or NHEJ to DNA damage and tumorigenesis in central nervous system (CNS) *in vivo,* we have compared the effects of germline disruption of either *Rad54* or *DNA–PKcs* on MB development in *Ptc1*$^{+/-}$ mice. To this aim, control and irradiated groups of *Ptc1*$^{+/-}$ mice with two, one or no intact *Rad54* or *DNA–PKcs* alleles were placed on a lifetime study for MB development. We discuss the functional interrelationship of HR and NHEJ in the processing of endogenous and radiation-induced DSBs, as well as in the molecular pathogenesis of cancer.

Results

Effect of Rad54 and DNA–PKcs inactivation on DNA damage in unirradiated and irradiated cerebellum at postnatal day 1 (P1)

DNA repair is critical for neural development, and defects in this process underlie neurological disease. Many human syndromes with DNA repair deficiency are, in fact, characterized by neuropathology, such as neurodegeneration, microcefaly or brain tumors, suggesting that responding to DNA DSBs is essential for neural homeostasis (McKinnon, 2009). Given the importance of *Ptc1* for CNS development and tumorigenesis, we sought to determine the potential relationship with DNA repair pathways. Although mouse studies are crucial for the analysis of cancer frequency, they are usually less informative for the dissection of end points, such as DSB processing and cell survival. The mouse cerebellum, however, is characterized by extended postnatal development, and the effects of inefficient HR or NHEJ on the processing of DNA damage can be detected and quantified *in vivo* (Pazzaglia *et al*., 2006b). Increasing evidence points to granule neuron precursors (GNPs) as the cells of origin of MB (Marino, 2005). Therefore, to assess the effect of NHEJ or HR inactivation on endogenous DNA damage, we examined γ-H2AX staining and apoptosis in GNPs of mice with combined inactivation of either *Rad54* or *DNA–PKcs* with *Ptc1* at P1, a stage when GNPs are clustered over the cerebellar surface to form the external granule layer (EGL). We found that inactivation of either *Rad54* or *DNA–PKcs* leads to abnormal levels of DSBs in GNPs, with *Rad54*- and *DNA–PKcs*-null mice showing a fivefold increased incidence of γ-H2AX-positive nuclei compared with wild-type (wt) mice (Figures 1a–c). Phosphorylation of H2AX marks a signaling cascade for the resolution of the break that may lead to its accurate repair, or to genomic rearrangements or apoptosis if the break is misrepaired or unrepaired. We therefore examined apoptotic cell death in GNPs. As an apoptotic marker, following confirmation by anti-activated-caspase-3 immunostaining, we evaluated the fraction of pyknotic nuclei in the EGL of mutant and wt mice (Figures 1d and e). Inhibition of *Rad54*-dependent specific HR events resulted in a fourfold increase in the rate of spontaneous apoptosis in neural precursors compared with wt mice ($P = 0.0417$) (Figures 1d and f). In addition, abundant apoptosis was found in the EGL of *DNA–PKcs* mutants, with a nearly sevenfold increase compared with wt mice ($P = 0.0002$) (Figures 1e and f). To exclude the possibility that *Rad54*- or *DNA–PKcs*-related increases in apoptosis might be due to differences in proliferation rate of neural precursors, we compared proliferation by proliferating-cell nuclear antigen immunostaining (PCNA) in the EGL from unirradiated cerebella at P1. We show no changes in the frequency of PCNA-positive cells in the EGL of *Rad54*$^{+/+}$/*Ptc1*$^{+/-}$ compared with *Rad54*$^{-/-}$/*Ptc1*$^{+/-}$ mice (85.2 vs 80.9%). There was also no difference between *DNA–PKcs*$^{+/+}$/*Ptc1*$^{+/-}$ and *DNA–PKcs*$^{-/-}$/*Ptc1*$^{+/-}$ mice (81.0 vs 81.8%; Figures 1g and h). In agreement with the γ-H2AX data, the increased neural apoptosis associated with HR or NHEJ deficiency supports a role for both these pathways in protecting the developing nervous system from endogenous DNA damage and apoptosis.

We next analyzed the effect of genotoxic stress by radiation in the neonatal cerebellum of mice with combined inactivation of either *Rad54* or *DNA–PKcs* and *Ptc1*. Compared with untreated mice, irradiation

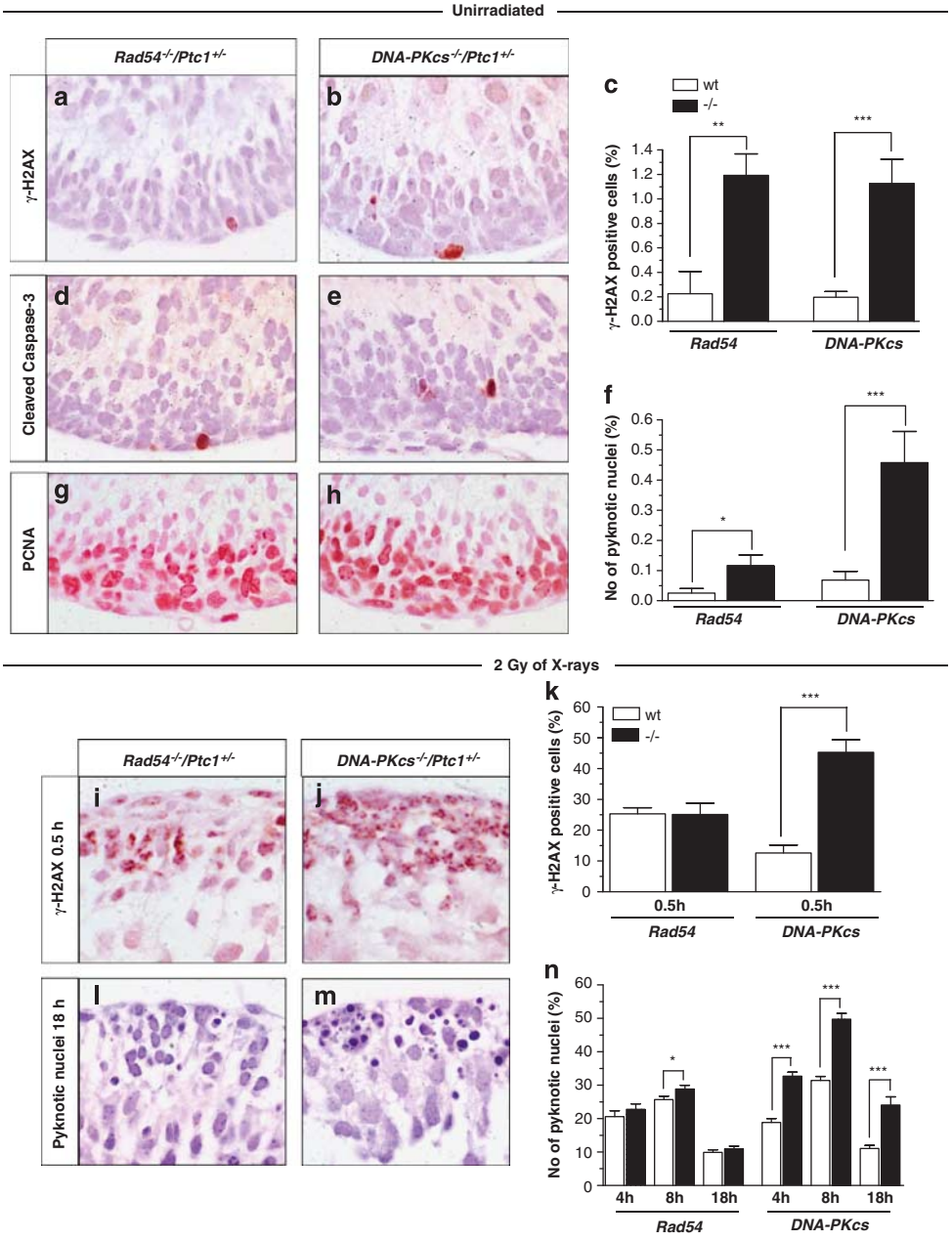

Figure 1 Effect of *Rad54* and *DNA–PKcs* genetic inactivation on DNA-damage response, apoptosis and proliferation in GNPs. Immunostaining against γ-H2AX (**a**, **b**), cleaved caspase-3 (**d**, **e**) and proliferating-cell nuclear antigen (PCNA) (**g**, **h**) in the cerebellum of unirradiated *Rad54*$^{-/-}$/*Ptc1*$^{+/-}$ and *DNA–PKcs*$^{-/-}$/*Ptc1*$^{+/-}$ mice. Quantification of endogenous DNA damage (**c**) and cell death (**f**) in GNPs from *Rad54*$^{-/-}$/*Ptc1*$^{+/-}$ and *DNA–PKcs*$^{-/-}$/*Ptc1*$^{+/-}$ mutants. (**i**, **j**) Immunostaining against γ-H2AX in the cerebellum of irradiated *Rad54*$^{-/-}$/*Ptc1*$^{+/-}$ and *DNA–PKcs*$^{-/-}$/*Ptc1*$^{+/-}$ mice at 0.5 h post irradiation, and (**k**) quantitative representation. (**l**, **m**) Representative hematoxylin and eosin-stained sections showing radiation-induced nuclear pyknosis in the EGL of *Rad54*$^{-/-}$/*Ptc1*$^{+/-}$ and *DNA–PKcs*$^{-/-}$/*Ptc1*$^{+/-}$ mice at 18 h post irradiation. (**n**) Quantitative representation of pyknotic nuclei (4, 8 and 18 h post irradiation) in the EGL. *$P \leqslant 0.05$; **$P \leqslant 0.005$; ***$P \leqslant 0.0001$.

with 2 Gy of X-rays at P1 caused a strong induction of γ-H2AX-positive GNPs in mice of all genotypes (Figures 1c and k). Irradiation of *Rad54*$^{-/-}$ mice did not modify the number of γ-H2AX-positive cells at 0.5 h post irradiation over the wt mice (Figures 1i and j). Instead, exposure of *DNA–PKcs*$^{-/-}$ mice caused a highly significant enhancement of 3.5-fold ($P < 0.0001$) (Figures 1i and k). We next analyzed the apoptotic response of GNPs in irradiated mice (Figure 1l). In *Rad54* mutants, an increase that reached statistical significance in apoptotic cell death was observed only at 8 h after irradiation (1.12-fold; $P = 0.0348$). In contrast, loss of *DNA–PKcs* function caused significant increases in apoptotic rates at all time points, with 1.7-fold, 1.6-fold, and 2.2-fold incidences at 4, 8, and 18 h, respectively ($P < 0.0001$). At 18 h after irradiation, a

large number of apoptotic bodies were still evident in the EGL of *DNA–PKcs*$^{-/-}$ mice compared with *Rad54*$^{-/-}$ and wt mice (Figures 1l–n). Collectively, these findings indicate a predominant function of NHEJ in processing radiation-induced DSBs and promoting survival of neural precursors of the developing cerebellum after DNA damage by radiation.

Survival and tumorigenesis in crosses between Ptc1 and Rad54 or DNA–PKcs mutant mice

To evaluate the effects of inactivation of either HR or NHEJ on survival and tumor response, groups of *Ptc1*$^{+/+}$ and *Ptc1*$^{+/-}$ mice of the different *Rad54* or *DNA–PKcs* genotypes were exposed to 2 Gy of X-rays at P1 or left untreated, and monitored for survival and tumor development.

First, we evaluated the effect of *Rad54* and *DNA–PKcs* deficiency on mouse survival. Compound mutants for *Ptc1* and *Rad54* or *DNA–PKcs* were viable, suggesting that combined deregulation of sonic hedgehog and DNA repair pathways is not critically important for normal development and survival. In unirradiated *Ptc1*$^{+/+}$ mice, homozygous deletion of *Rad54* did not modify survival relative to *Rad54*$^{+/+}$ mice (105 vs 109 weeks; $P=0.995$) (Figure 2a). In contrast, lack of *Rad54* conferred a marked radiosensitive phenotype, with significant life shortening observed in irradiated *Rad54*$^{-/-}$/*Ptc1*$^{+/+}$ mice compared with unexposed mice of the same genotype (84 vs 105 weeks; $P<0.0001$), or with irradiated *Rad54*$^{+/+}$/*Ptc1*$^{+/+}$ mice (84 vs 93 weeks; $P=0.0147$) (Figure 2a). This life shortening was mainly due to a significant increase in thymic lymphoma (22.2% in *Rad54*$^{-/-}$/*Ptc1*$^{+/+}$ mice vs 9.5% in *Rad54*$^{+/+}$/*Ptc1*$^{+/+}$ mice; $P=0.0437$). Inactivation of a *Ptc1* copy *per se* caused a sharp reduction in median survival compared with *Ptc1*$^{+/+}$ mice (53 vs 109 weeks; $P=0.0028$) (Figures 2a and b). In *Ptc1*$^{+/-}$ mice, irradiation caused further life shortening compared with unirradiated mice (35 vs 53 weeks; $P=0.0093$), and this effect was markedly affected by the *Rad54* status (20.5 vs 35 weeks; $P=0.0088$) (Figure 2b). Importantly, our data show for the first time an overt radiosensitive phenotype of *Rad54* mutant mice when challenged with ionizing radiation as newborns. Consistent with previous results (Essers *et al*., 1997), *Rad54*$^{-/-}$ mice are not radiosensitive in the short term, but apparently, repair of certain radiation-induced DNA lesions by *Rad54*-mediated HR contributes to long-term survival.

In unexposed *Ptc1*$^{+/+}$ mice, loss of *DNA–PKcs* function significantly reduced mouse lifespan compared with *DNA–PKcs*$^{+/+}$ mice, due to early onset of aging-related pathologies (Espejel *et al*., 2004) (17 vs 107 weeks, $P<0.0001$) (Figure 2c), and irradiation did not cause further reduction of survival. Inactivation of a copy of the *Ptc1* gene caused a sharp reduction of median survival in unexposed *Ptc1*$^{+/-}$ mice compared with *Ptc1*$^{+/+}$ mice (62 vs 107 weeks; $P=0.0002$) (Figures 2c and d). Irradiation of *Ptc1*$^{+/-}$ mice induced a drastic life shortening compared with untreated mice of the matching genotype (17 vs 62 weeks; $P<0.0001$), and this effect was more severe in *DNA–PKcs*$^{-/-}$ mice (11 vs 17 weeks; $P=0.0002$) (Figure 2d).

Because only *Ptc1*$^{+/-}$ mice are prone to MB, the effects of *Rad54* and *DNA–PKcs* inactivation on CNS tumor response were evaluated in *Ptc1*$^{+/-}$ mice of the three *Rad54* and *DNA–PKcs* genotypes. There was no statistically significant difference in spontaneous MB incidence between *Rad54*$^{+/+}$/*Ptc1*$^{+/-}$ and *Rad54*$^{-/-}$/*Ptc1*$^{+/-}$ mice, although *Rad54* deletion caused a trend towards increased MB development, and differences approached statistical significance between mice with homozygous or heterozygous *Rad54* deletion (6/18, (33.3%) vs 3/29, (10.3%); $P=0.067$) (Figure 3a). Notably, irradiation significantly increased MB development in *Rad54*$^{-/-}$/*Ptc1*$^{+/-}$ mice compared with *Rad54*$^{+/+}$/*Ptc1*$^{+/-}$ mice (26/35 (74%) vs 10/23 (44%); $P=0.027$) (Figure 3b), showing a role for HR in protection from radiation-induced genotoxic damage leading to MB. Therefore, despite a mild phenotype regarding apoptotic cell death in the developing cerebellum, deletion of *Rad54* significantly increased MB tumorigenesis, likely through the generation of viable but genetically rearranged neural precursors that may represent a vulnerable cell pool *en route* to MB. In line with this, evidence from the literature shows that *Rad54* inactivation results in increased rates of spontaneous chromosome loss in diploid cells in *Saccharomyces cerevisiae* and in various spontaneous chromosome aberrations in DT-40 cells (Wang *et al*., 2000; Schmuckli-Maurer *et al*., 2003).

Significantly, *DNA–PKcs* deletion caused a suppression of spontaneous MB, with complete lack of tumors in the *DNA–PKcs*$^{-/-}$/*Ptc1*$^{+/-}$ group. This result was significantly different from *DNA–PKcs*$^{+/-}$/*Ptc1*$^{+/-}$ mice (0/20, (0%) vs 7/33, (21.2%); $P=0.037$), although not statistically significant compared with *DNA–PKcs*$^{+/+}$/*Ptc1*$^{+/-}$ mice (Figure 3c). In addition, irradiation significantly decreased MB development in *DNA–PKcs*$^{-/-}$ mice (7/18 (38.8%) vs 41/53 (77.4%); $P=0.0072$) (Figure 3d). Because the rapid decline of mouse health and lifespan in *DNA–PKcs* mutants may have prevented MB development, we sought to analyze early MB stages in the cerebella of *DNA–PKcs*$^{+/+}$/*Ptc1*$^{+/-}$ and *DNA–PKcs*$^{-/-}$/*Ptc1*$^{+/-}$ mice at 5 weeks, when mortality rates are still low (Figure 3e). Such early MB microscopic lesions are a typical feature of the cerebellum of young *Ptc1*$^{+/-}$ mice and are considered suggestive of a preneoplastic condition (Pazzaglia *et al*., 2002; Oliver *et al*., 2005; Tanori *et al*., 2008). There was a modest decrease in spontaneous MB microscopic lesions in *DNA–PKcs*$^{-/-}$/*Ptc1*$^{+/-}$ mice relative to *DNA–PKcs*$^{+/+}$/*Ptc1*$^{+/-}$ mice (7/13 (54%) vs 7/16 (44%)). After irradiation, this trend became more evident, with a 1.5-fold difference (9/17 (53%) vs 16/20 (80%)). A 1.4-fold lower incidence of MB microscopic lesions was also observed in *DNA–PKcs*$^{+/-}$/*Ptc1*$^{+/-}$ compared with *DNA–PKcs*$^{+/+}$/*Ptc1*$^{+/-}$mice (Figure 3e). Therefore, the high apoptotic levels observed in *DNA–PKcs* null mice (Figures 1m and n) might represent a protective mechanism that prevents the accumulation of oncogenic DNA damage in the developing cerebellum.

Effects of *Rad54* inactivation on survival

a

Dose	*Ptc1*$^{+/+}$	Mice	Median survival (weeks)
0 Gy	*Rad54*$^{+/+}$	19	109.0
	Rad54$^{+/-}$	28	110.5
	Rad54$^{-/-}$	27	105.0 [a]
2 Gy	*Rad54*$^{+/+}$	24	93.0 [b]
	Rad54$^{+/-}$	18	89.0
	Rad54$^{-/-}$	29	84.0 [c]

* b-c and *** a-c in the Log rank test

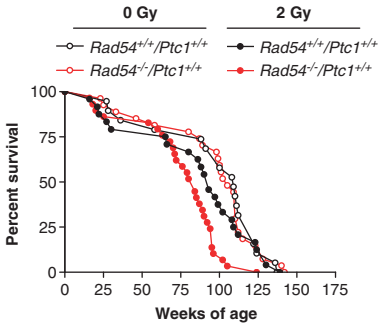

b

Dose	*Ptc1*$^{+/-}$	Mice	Median survival (weeks)
0 Gy	*Rad54*$^{+/+}$	22	53.0 [a]
	Rad54$^{+/-}$	31	84.0 [b]
	Rad54$^{-/-}$	18	33.5 [c]
2 Gy	*Rad54*$^{+/+}$	24	35.0 [d]
	Rad54$^{+/-}$	33	24.0 [e]
	Rad54$^{-/-}$	36	20.5 [f]

** a-d, c-f and d-f, *** b-e in the Log rank test

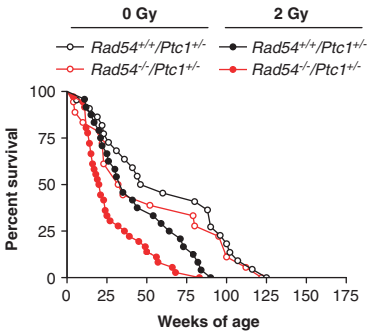

Effects of *DNA-PKcs* inactivation on survival

c

Dose	*Ptc1*$^{+/+}$	Mice	Median survival (weeks)
0 Gy	*DNA-PK*$_{cs}^{+/+}$	24	107.0 [a]
	DNA-PK$_{cs}^{+/-}$	24	89.5 [b]
	DNA-PK$_{cs}^{-/-}$	10	17.0 [c]
2 Gy	*DNA-PK*$_{cs}^{+/+}$	46	97.0 [d]
	DNA-PK$_{cs}^{+/-}$	46	91.0 [e]
	DNA-PK$_{cs}^{-/-}$	24	12.5 [f]

* a-b; ** e-f , ***a-c, b-c, and d-f in the Log rank test

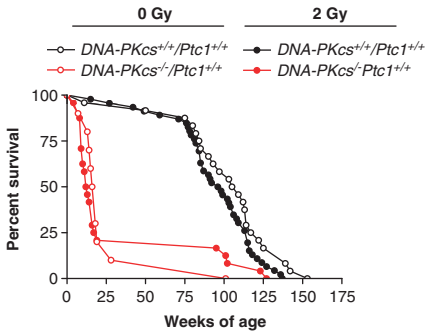

d

Dose	*Ptc1*$^{+/-}$	Mice	Median survival (weeks)
0 Gy	*DNA-PKcs*$^{+/+}$	32	62.0 [a]
	DNA-PKcs$^{+/-}$	34	63.5 [b]
	DNA-PKcs$^{-/-}$	23	17.0 [c]
2 Gy	*DNA-PKcs*$^{+/+}$	58	17.0 [d]
	DNA-PKcs$^{+/-}$	72	21.0 [e]
	DNA-PKcs$^{-/-}$	24	11.0 [f]

*** a-d, b-e, e-f, c-f and d-f in the Log rank test

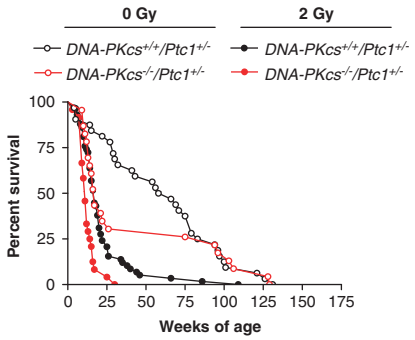

Figure 2 Survival of unirradiated and irradiated *Ptc1* mice with two, one or no intact *Rad54* or *DNA–PKcs* alleles. (**a**) Group size and median survival of unirradiated and irradiated *Ptc1*$^{+/+}$ and (**b**) *Ptc1*$^{+/-}$ mice with two, one or no functional *Rad54* alleles, and graphic representation of survival over time for the extreme genotypes. (**c**) Group size and median survival of unirradiated and irradiated *Ptc1*$^{+/+}$ and (**d**) *Ptc1*$^{+/-}$ mice with two, one or no intact *DNA–PKcs* alleles, and graphic representation of survival over time for the extreme genotypes.

Biallelic *Ptc1* loss has a fundamental role in progression of MB preneoplasia (Pazzaglia *et al*., 2006a). Therefore, preneoplastic lesions from single and compound mutants were microdissected by laser capture and assayed for loss of the wt *Ptc1* allele (Figures 3f–i). We show that biallelic *Ptc1* loss is a frequent event, occurring in 75–100% of spontaneous and radiation-induced preneoplastic lesions arising in *DNA–PKcs*$^{+/+}$/*Ptc1*$^{+/-}$ and *DNA–PKcs*$^{+/-}$/*Ptc1*$^{+/-}$ mice (Figure 3j). Interestingly, the rate of *Ptc1* LOH appeared to be decreased in preneoplastic lesions from unirradiated (1/2 vs 3/4) and irradiated (1/4 vs 4/5) *DNA–PKcs*$^{-/-}$ mice (Figure 3l), although these differences were not significant due to the

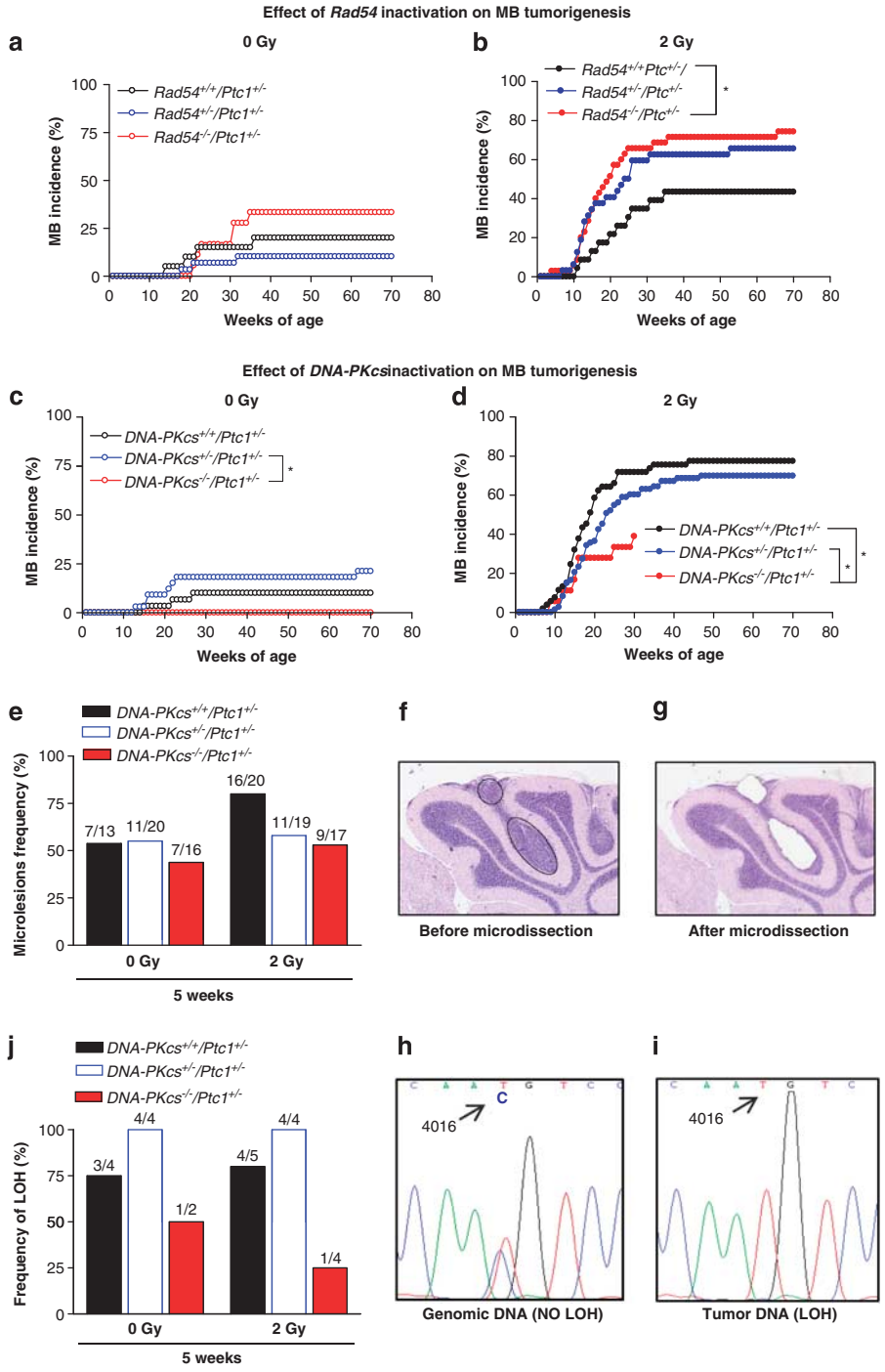

Figure 3 MB tumorigenesis in unirradiated and irradiated *Ptc1* mice with two, one or no functional *Rad54* or *DNA–PKcs* alleles. (**a**) MB development in unirradiated and (**b**) irradiated $Ptc1^{+/-}$ mice of the three *Rad54* genotypes. (**c**) MB development in unirradiated and (**d**) irradiated $Ptc1^{+/-}$ mice of the three *DNA–PKcs* genotypes. (**e**) Incidence of microscopic cerebellar lesions in unirradiated ($n=49$) and neonatally irradiated ($n=56$) $Ptc1^{+/-}$ mice with two, one or no functional *DNA–PKcs* alleles. (**f**, **g**) Representative laser-captured section of preneoplastic cerebellar lesion before (**f**) and after (**g**) microdissection. (**h**) Representative electropherogram of genomic DNA showing a polymorphism at position 4016 (arrows) for the presence of both CD1- (C) and 129Sv-derived (T) nucleotides, demonstrating retention of wt and mutated alleles in normal tissue. (**i**) Electropherogram of DNA extracted from a preneoplastic lesion showing only the 129Sv allele (T), demonstrating loss of wt *Ptc1*. (**j**) Frequency of LOH at the *Ptc1* locus in cerebellar preneoplastic lesions microdissected from unirradiated ($n=10$) and irradiated ($n=13$) $Ptc1^{+/-}$ mice of the three *DNA–PKcs* genotypes.

small sample size. Collectively, these data show that loss of *DNA–PKcs* function decreases the frequency of early and late MB stages, as well as the rate of biallelic *Ptc1* loss in MB microscopic lesions, suggesting an involvement of NHEJ in LOH events in the cerebellum.

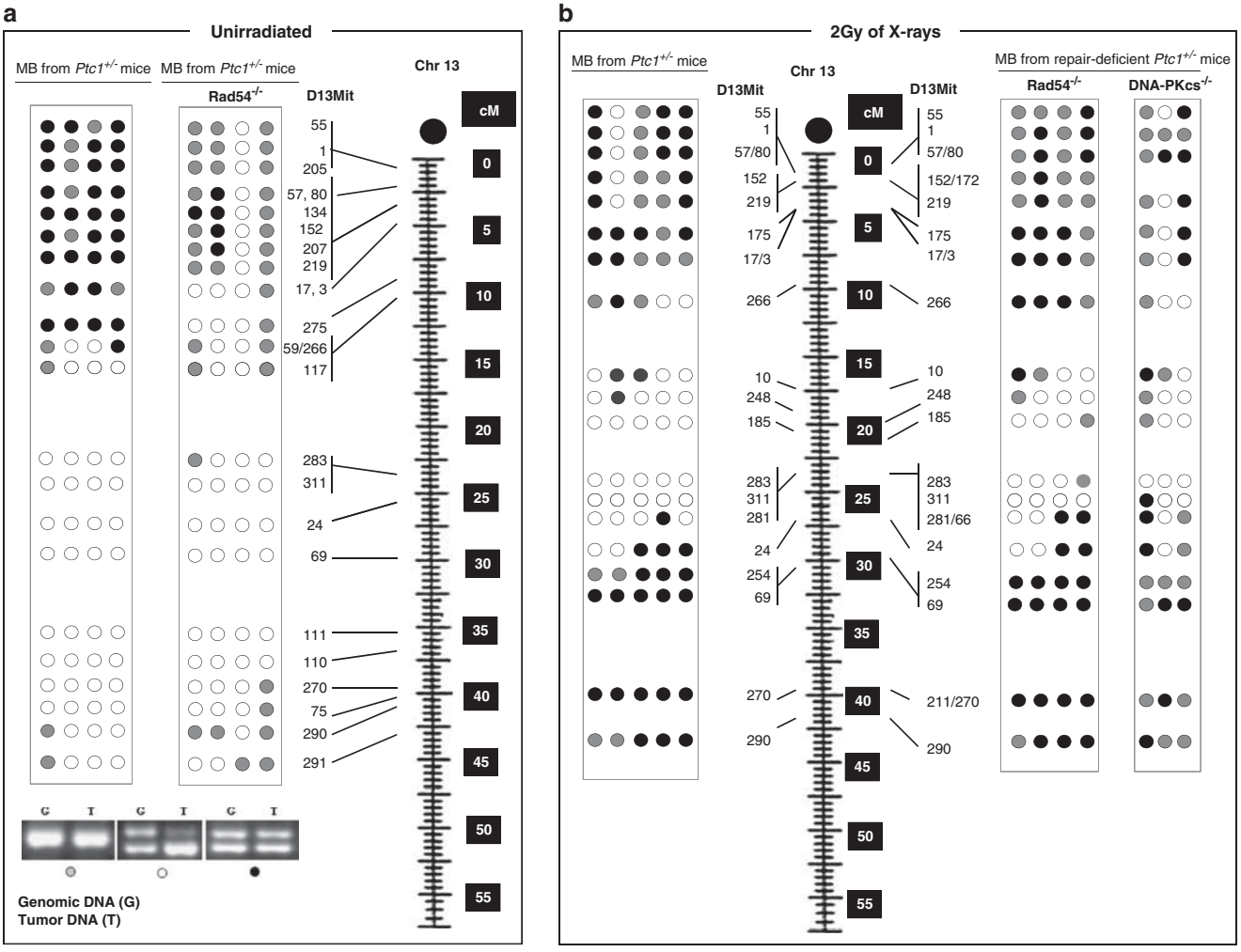

Figure 4 Analysis of chromosome 13 LOH in spontaneous and radiation-induced MBs from *Ptc1*$^{+/-}$ mice with two or no intact *Rad54* or *DNA–PKcs* alleles. (**a**) MB from unirradiated or (**b**) X-ray-exposed mice. The distance of microsatellite markers (D13Mit) from the centromere is given in cM, with values taken from the Genetic and Physical Maps of the Mouse Genome (1999). Black circles indicate no loss of PCR signal from either allele; open circles denote loss of signal from one allele (LOH); gray circles indicate not informative (NI) markers. PCR primers were purchased from Research Genetics (Huntsville, AL, USA).

Effect of Rad54 and DNAPKcs deficiency on Ptc1 LOH in full-blown MBs

We went on to examine *Ptc1* LOH in fully developed tumors. Spontaneous and radiation-induced MBs from single (*Ptc1*) and compound mutants (*Rad54* or *DNA–PKcs*) were examined with a set of microsatellite markers spanning the length of chromosome 13, where the *Ptc1* gene is located (Figure 4). Lack of spontaneous MBs prevented analysis in *DNA–PKcs*$^{-/-}$/*Ptc1*$^{+/-}$ mutants. In agreement with previous data (Pazzaglia *et al*., 2006a), all spontaneous MBs from *Ptc1*$^{+/-}$ mice ($n=4$) showed a typical pattern of *Ptc1* LOH involving loss of a large terminal region of chromosome 13. In MBs from *Rad54*$^{-/-}$/*Ptc1*$^{+/-}$ mice, two out of four tumors showed this typical pattern. Of the two remaining MBs, one showed whole-chromosome 13 loss, whereas the other was undetermined because of lack of polymorphism of many critical markers (Figure 4a). Although these findings might suggest that the LOH mechanism in spontaneous tumors can be influenced by *Rad54* inactivation, the sample size was too small to justify any mechanistic hypothesis. However, increased frequency of aneuplody, related to centrosome abnormalities, has also been observed in cells defective for other recombination genes such as *BRCA1*, *BRCA2*, *XRCC2*, *XRCC3* and *Rad51* paralogue family (Tutt *et al*., 1999; Xu *et al*., 1999; Griffin *et al*., 2000; Deans *et al*., 2003; Yoshihara *et al*., 2004; Smiraldo *et al*., 2005).

In radiation-induced MBs, the pattern of *Ptc1* LOH was distinct from that of spontaneous tumors, as previously observed (Pazzaglia *et al*., 2006a). All radiogenic MBs showed large interstitial chromosome 13 deletions, suggesting different molecular mechanisms for spontaneous or radiation-induced *Ptc1* loss (Figure 4b). However, within the sample size analyzed, no obvious difference in the pattern of *Ptc1* LOH was observed following genetic inactivation of *Rad54* or *DNA–PKcs*.

Discussion

Collectively, our data support the hypothesis that a balanced interplay between HR and NHEJ deficiencies is essential to maintain genomic integrity and suppress tumorigenesis in the developing mouse CNS, with or without exogenous DNA damage by radiation. Competition between HR and NHEJ in processing DSBs may help explain the decreased MB incidence in *DNA–PKcs*$^{-/-}$/*Ptc1*$^{+/-}$ mice. In fact, HR may compensate for deficiency in NHEJ in *DNA–PKcs* mutants, resulting in increased genome stability. This is a likely scenario as *DNA–PKcs* is known to suppress HR of induced and spontaneous DSBs (Allen *et al*., 2002) by protecting DNA ends from the initial resection steps necessary for HR (Sung 1994; Baumann *et al*., 1996). On the other hand, HR has been reported to be increased in NHEJ mutants (Pellicioli *et al*., 2001; Pierce *et al*., 2001; Weinstock and Jasin, 2006). Support for an interplay between repair systems comes from our previous data showing that deletion of PARP-1—a good candidate for limiting the access of Ku to DSBs in favor of HR—mimics the effect of *Rad54* deletion, accelerating *Ptc1*-associated tumors (Tanori *et al*., 2008). Further evidence of HR and NHEJ interplay was suggested by studies of double mutant mice, in which *Rad54* deletion dramatically increased radiation sensitivity of NHEJ mutants (Essers *et al*., 2000; Couëdel *et al*., 2004; Mills *et al*., 2004).

The suppression of MB tumorigenesis in mice with *DNA–PKcs* inactivation was unexpected because mice with disruption of NHEJ components (DNA ligase IV, XRCC4, Ku80, artemis) in collaboration with defective p53 (Lee and McKinnon, 2002; Rooney *et al*., 2004; Holcomb *et al*., 2006; Yan *et al*., 2006) are prone to MB. Nevertheless, Ku80-deficient mice exhibited low cancer levels (Vogel *et al*., 1999; Li *et al*., 2007), and deleting Ku80 in *Apc*$^{(min/+)}$ mice decreased intestinal tumorigenesis (Holcomb *et al*., 2008). Thus, deletion of NHEJ components might increase tumorigenesis only in a p53-mutant background, dependent on the abrogation of p53 surveillance mechanisms. This hypothesis is supported by the observation that although microcefaly, growth delay and dysmorphic facial features are observed in some NHEJ-defective patients, no increased risk for brain tumors has been reported so far. Instead, mutations in HR repair factors, such as *BRCA2* and *NBS*, responsible of Fanconi anemia D1 (biallelic inheritance of *BRCA2* mutations) and Nijmegen breakage syndrome, predispose to MB, strengthening the association between inefficient HR and development of brain tumors (Bakhshi *et al*., 2003; Offit *et al*., 2003). Several lines of evidence also link missense mutations of the human *Rad54* gene to lymphoma, breast and colon cancer, suggesting a tumor suppressive function for this gene (Matsuda *et al*., 1999).

Our data provide the first *in vivo* experimental evidence that the distinct activities of DSBs repair pathways may differentially affect cancer risk by radiation. Of note, a strong correlation between polymorphysms/haplotypes of the *RAD51L1* gene and a γ-radiation sensitive phenotype in glioma patients has recently been identified, supporting the notion that inability to repair DSBs by HR increases sensitivity to γ-radiation and promotes brain tumorigenesis in humans (Liu *et al*., 2010).

In summary, germinal inactivation of *Rad54* and *DNA–PKcs* genes had opposite modifying effects on CNS tumorigenesis in mice, despite the common role of these genes in protecting neural precursors from endogenous and exogenous DNA damage. By providing evidence that loss of *Rad54* function increases brain tumor susceptibility in a well-established animal model of MB, our data also highlight a tumor suppressor function for *Rad54 in vivo*. In contrast, *DNA–PKcs* may promote *Ptc1*-associated MB tumorigenesis, likely through the joining of DNA breaks into chromosome rearrangements. Together, our *in vivo* data help to clarify the relative contribution of HR and NHEJ DNA damage response pathways to spontaneous and radiation-induced CNS tumorigenesis by showing that factors that modify HR proficiency, such as *Rad54,* may contribute to the origin of 'spontaneous' and therapy-related 'secondary' human cancers when mutated.

Materials and methods

Animal breeding

Mice lacking one *Ptc1* allele (*Ptc1*$^{neo6-7/+}$, named *Ptc1*$^{+/-}$ throughout the text) generated through disruption of exons 6 and 7 in 129/Sv embryonic stem cells (Hahn *et al*., 1998) and maintained on CD1 background were crossed with *Rad54*$^{-/-}$ (Essers *et al*., 1997) and *DNA–PKcs*$^{-/-}$ (Taccioli *et al*., 1998) mice maintained on C57B/6 background. F1 mice of the desired genotypes (*DNA–PKcs*$^{+/-}$/*Ptc1*$^{+/-}$ × *DNA–PKcs*$^{+/-}$/*Ptc1*$^{+/+}$ and *Rad54*$^{+/-}$/*Ptc1*$^{+/-}$ × *Rad54*$^{+/-}$/*Ptc1*$^{+/+}$) were intercrossed to produce large F2 populations. Genotyping of mice was by PCR of DNA isolated by tail clip. The PCR primers for *DNA–PKcs* were as follows: MQ7, 5′-AGA CTG GCT GAT GAA AGT GTC-3′; MQ3, 5′-TGA AAT TGT TCA GGT GTC TGT-3′; PK-Neo-R, 5′-CGG TGG ATG TGG AAT GTG TGC G-3′; DNA PK 62, 5′-AAG CGA TGC TGG AGC CTA TGT G-3′. The primers MQ7 and MQ3 amplify an ∼1000 bp fragment of the wt allele, whereas PK-Neo-R and DNA PK 62 amplify an ∼700 bp fragment of the targeted allele. The PCR primers for *Rad54* were 54KO1, 5′-AAG GAA GCA TTT ATT CGA AGT ATT T-3′; 54KO2, 5′-TTT GCT TCC TCT TGC AAA CCA-3′; 15M, 5′-GTT CAA AGC CAG TCA GCC TAG-3′. Fragments of ∼180 and ∼260 bp are obtained from the wt and targeted allele, respectively. Genotyping for *Ptc1* was performed as described previously (Hahn *et al*., 1998).

Animal treatment and irradiation

Mice were housed under conventional conditions with food and water available *ad libitum* and a 12-h light cycle. Mice were irradiated at P1 with 2 Gy of X-rays from a Gilardoni CHF 320 G X-ray generator (Gilardoni S.p.A., Lecco, Italy) operated at 250 kVp, 15 with filters of 2.0 mm Al and 0.5 mm Cu (half-value layer (HVL) = 1.6 mm Cu). Experimental protocols were reviewed by the Institutional Animal Care and Use Committee.

Histological analysis and tumor quantification
Mice were observed daily for their lifespan. Upon decline of health (that is, severe weight loss, paralysis, ruffling of fur or inactivity), they were killed and autopsied. Normally appearing and tumor-bearing brains were fixed in 4% buffered formalin. Samples were processed for histological analysis using standard methods. MB incidence was expressed as the percentage of mice with tumors. The incidence of preneoplastic cerebellar lesions was determined on histological sections of 5-week old asymptomatic $Ptc1^{+/-}$ mice with two, one or no functional *DNA–PKcs* alleles, irradiated at P1 or left untreated. In all, 18 sections, recovered with intervals of 70 μm to ensure representative sampling, were examined for each cerebellum.

Radiosensitivity analysis
Brains (three per time point) from irradiated $Ptc1^{+/-}$ pups with two, one or no functional *DNA–PKcs* or *Rad54* alleles were collected at 4, 8 and 18 h post irradiation and fixed in 4% buffered formalin. Brains from unirradiated pups ($n = 3$) were also examined. Serial sections of cerebellar tissues were cut at 4-μm thickness and stained with hematoxylin and eosin. Digital images from midsagittal cerebellar sections, covering the entire EGL, were collected by IAS image-processing software (Delta Sistemi, Rome, Italy). Cells showing signs of nuclear chromatin condensation and morphologically normal cells in the EGL were counted using a double-blind method. Cell death was calculated as the percentage pyknotic nuclei relative to the total number of cells.

Immunohistochemical analysis
Immunohistochemical analysis was carried out as described (Tanori *et al*., 2008). Antibodies used were as follows: rabbit polyclonal antibody against cleaved caspase-3 (Cell Signaling Technology, Denvers, MA, USA), monoclonal antibody against proliferating-cell nuclear antigen (Calbiochem, Darmstadt, Germany), and γ-H2AX (Upstate Biotechnology, Lake Placid, NY, USA). To investigate kinetics of γ-H2AX in GNPs *in situ*, cerebella from $Ptc1^{+/-}$ pups with two, one or no intact *DNA–PKcs* or *Rad54* alleles were collected at 0.5 h post irradiation. Percentage of γ-H2AX-positive nuclei in the entire EGL from sagittal sections of cerebellum (three per time point) were counted using a double-blind method. The number of cells with γ-H2AX foci was calculated as the percentage of positive cells relative to the total number of cells.

Microsatellite analysis at the Ptc1 locus
DNA was extracted from MB and normal tissue using Wizard SV Genomic DNA Purification System (Promega Corporation, Madison, WI, USA). A typical PCR experiment involved analysis of DNAs from tumors and corresponding genomic DNA as control. PCR amplifications were performed as described previously (Pazzaglia *et al*., 2000). About 20 microsatellites spanning the length of chromosome 13 were used to examine MBs from $DNA\text{–}PKcs^{+/+}/Ptc1^{+/-}$, $DNA\text{–}PKcs^{-/-}/Ptc1^{+/-}$, $Rad54^{+/+}/Ptc1^{+/-}$ and $Rad54^{-/-}/Ptc1^{+/-}$ irradiated and unirradiated mice.

LOH at the Ptc1 locus in preneoplastic lesions
Preneoplastic areas in cerebellum from unirradiated and irradiated $DNA\text{–}PKcs^{+/+}/Ptc1^{+/-}$ and $DNA\text{–}PKcs^{-/-}/Ptc1^{+/-}$ were microdissected with a laser microscope system (P.A.L.M., Wolfratshausen, Germany) consisting of a Zeiss Axiovert microscope (Zeiss, Jena, Germany), a pulsed UV-laser (wavelength 337 nm, maximum frequency: 20 pulses/s, pulse duration: 3 ns) and a computer-controlled micromanipulator. DNAs from microdissected cerebellar lesions were extracted with PicoPure DNA extraction Kit (Arcturus, CA, USA) and subjected to nested-PCR as described (Pazzaglia *et al*., 2006a, b). The product of PCR was purified (Wizard SV gel and PCR Clean-Up System, Promega) and sequenced. Sequencing reactions were performed by means of dye terminator chemistry using a Big Dye Terminator Version 3.1 Sequencing Cycle Kit and 3730 DNA Analyzer (Applied Biosystems, Foster City, CA, USA). The presence of both CD1- (C) and 129Sv-derived (T) polymorphisms at position 4016 demonstrates retention of both *Ptc1* alleles, whereas the presence of a unique peak corresponding to the 129Sv allele (T) represents loss of the wt *Ptc1* allele.

Statistics
Analyses were performed using GraphPad Prism version 4.02 for Windows (GraphPad Software, San Diego, CA, USA). Proliferation and apoptotic indexes are reported as means ± s.e., and the Student's *t*-test was used for determination of statistical difference between groups. Log-rank test was used for determination of statistical differences in percent survival between groups, and Fisher's exact test for analysis of tumor incidence. *P*-value <0.05 was considered statistically significant.

Conflict of interest

The authors declare no conict of interest.

Acknowledgements

This work was supported by EU Contract FI6R-CT-2003-508842 RISC-RAD, by Grant 10357 from the Associazione Italiana Ricerca sul Cancro (AIRC) and the Netherlands Genomics Initiative/Netherlands Organization for Scientific Research.

References

Allen C, Kurimasa A, Brenneman MA, Chen DJ, Nickoloff JA. (2002). DNA-dependent protein kinase suppresses double-strand break-induced and spontaneous homologous recombination. *Proc Natl Acad Sci USA* **99**: 3758–3763.

Bakhshi S, Cerosaletti KM, Concannon P, Bawle EV, Fontanesi J, Gatti RA *et al*. (2003). Medulloblastoma with adverse reaction to radiation therapy in nijmegen breakage syndrome. *J Pediatr Hematol Oncol* **25**: 248–251.

Baumann P, Benson FE, West SC. (1996). Human Rad51 protein promotes ATP-dependent homologous pairing and strand transfer reactions *in vitro*. *Cell* **87**: 757–766.

Cahill D, Connor B, Carney JP. (2006). Mechanisms of eukaryotic DNA double strand break repair. *Front Biosci* **11**: 1958–1976.

Couëdel C, Mills KD, Barchi M, Shen L, Olshen A, Johnson RD *et al*. (2004). Collaboration of homologous recombination and nonhomologous end-joining factors for the survival and integrity of mice and cells. *Genes Dev* **18**: 1293–1304.

Deans B, Griffin CS, O'Regan P, Jasin M, Thacker J. (2003). Homologous recombination deficiency leads to profound genetic instability in cells derived from Xrcc2-knockout mice. *Cancer Res* **63**: 8181–8187.

Espejel S, Martín M, Klatt P, Martín-Caballero J, Flores JM, Blasco MA. (2004). Shorter telomeres, accelerated ageing and increased lymphoma in DNA-PKcs-deficient mice. *EMBO Rep* **5**: 503–509.

Essers J, Hendriks RW, Swagemakers SM, Troelstra C, de Wit J, Bootsma D *et al*. (1997). Disruption of mouse RAD54 reduces ionizing radiation resistance and homologous recombination. *Cell* **89**: 195–204.

Essers J, van Steeg H, de Wit J, Swagemakers SM, Vermeij M, Hoeijmakers JH *et al*. (2000). Homologous and non-homologous recombination differentially affect DNA damage repair in mice. *EMBO J* **19**: 1703–1710.

Frappart PO, Lee Y, Lamont J, McKinnon PJ. (2007). BRCA2 is required for neurogenesis and suppression of medulloblastoma. *EMBO J* **26**: 2732–2742.

Frappart PO, Lee Y, Russell HR, Chalhoub N, Wang YD, Orii KE *et al*. (2009). Recurrent genomic alterations characterize medulloblastoma arising from DNA double-strand break repair deficiency. *Proc Natl Acad Sci USA* **106**: 1880–1885.

Griffin CS, Simpson PJ, Wilson CR, Thacker J. (2000). Mammalian recombination-repair genes XRCC2 and XRCC3 promote correct chromosome segregation. *Nat Cell Biol* **2**: 757–761.

Hahn H, Wojnowski L, Zimmer AM, Hall J, Miller G, Zimmer A. (1998). Rhabdomyosarcomas and radiation hypersensitivity in a mouse model of Gorlin syndrome. *Nat Med* **4**: 619–622.

Holcomb VB, Rodier F, Choi Y, Busuttil RA, Vogel H, Vijg J *et al*. (2008). Ku80 deletion suppresses spontaneous tumors and induces a p53-mediated DNA damage response. *Cancer Res* **68**: 9497–9502.

Holcomb VB, Vogel H, Marple T, Kornegay RW, Hasty P. (2006). Ku80 and p53 suppress medulloblastoma that arise independent of Rag-1-induced DSBs. *Oncogene* **25**: 7159–7165.

Lee Y, McKinnon PJ. (2002). DNA ligase IV suppresses medulloblastoma formation. *Cancer Res* **62**: 6395–6399.

Levanat S, Gorlin RJ, Fallet S, Johnson DR, Fantasia JE, Bale AE. (1996). A two-hit model for developmental defects in Gorlin syndrome. *Nat Genet* **12**: 85–87.

Li H, Vogel H, Holcomb VB, Gu Y, Hasty P. (2007). Deletion of Ku70, Ku80, or both causes early aging without substantially increased cancer. *Mol Cell Biol* **27**: 8205–8214.

Li X, Heyer WD. (2008). Homologous recombination in DNA repair and DNA damage tolerance. *Cell Res* **1**: 99–113.

Liu Y, Shete S, Wang LE, El-Zein R, Etzel CJ, Liang FW *et al*. (2010). Gamma-radiation sensitivity and polymorphisms in RAD51L1 modulate glioma risk. *Carcinogenesis* **31**: 1762–1769.

Mancuso M, Pazzaglia S, Tanori M, Hahn H, Merola P, Rebessi S *et al*. (2004). Basal cell carcinoma and its development: insights from radiation-induced tumors in *Ptch1*-deficient mice. *Cancer Res* **3**: 934–941.

Marino S. (2005). Medulloblastoma: developmental mechanisms out of control. *Trends Mol Med* **11**: 17–22.

Matsuda M, Miyagawa K, Takahashi M, Fukuda T, Kataoka T, Asahara T *et al*. (1999). Mutations in the RAD54 recombination gene in primary cancers. *Oncogene* **18**: 3427–3430.

McKinnon PJ. (2009). DNA repair deficiency and neurological disease. *Nat Rev Neurosci* **10**: 100–112.

Mills KD, Ferguson DO, Essers J, Eckersdorff M, Kanaar R, Alt FW. (2004). Rad54 and DNA ligase IV cooperate to maintain mammalian chromatid stability. *Genes Dev* **18**: 1283–1292.

Moynahan ME, Jasin M. (1997). Loss of heterozygosity induced by a chromosomal double-strand break. *Proc Natl Acad Sci USA* **19**: 948988–948993.

Offit K, Levran O, Mullaney B, Mah K, Nafa K, Batish SD *et al*. (2003). Shared genetic susceptibility to breast cancer, brain tumors, and Fanconi anemia. *J Natl Cancer Inst* **95**: 1548–1551.

Oliver TG, Read TA, Kessler JD, Mehmeti A, Wells JF, Huynh TT *et al*. (2005). Loss of patched and disruption of granule cell development in a pre-neoplastic stage of medulloblastoma. *Development* **132**: 2425–2439.

Pazzaglia S, Mancuso M, Atkinson MJ, Tanori M, Rebessi S, Di Majo V *et al*. (2002). High incidence of medulloblastoma following X-ray-irradiation of newborn Ptc1 heterozygous mice. *Oncogene* **49**: 7580–7584.

Pazzaglia S, Pariset L, Rebessi S, Saran A, Coppola M, Covelli V *et al*. (2000). Somatic cell hybrids for high-density mapping of chromosome 2 breakpoints in radiation-induced myeloid leukemia cell lines from inbred mice. *Mol Carcinog* **27**: 219–228.

Pazzaglia S, Tanori M, Mancuso M, Gessi M, Pasquali E, Leonardi S *et al*. (2006a). Two-hit model for progression of medulloblastoma preneoplasia in patched heterozygous mice. *Oncogene* **40**: 5575–5580.

Pazzaglia S, Tanori M, Mancuso M, Rebessi S, Leonardi S, Di Majo V *et al*. (2006b). Linking DNA damage to medulloblastoma tumorigenesis in patched heterozygous knockout mice. *Oncogene* **25**: 1165–1173.

Pellicioli A, Lee SE, Lucca C, Foiani M, Haber JE. (2001). Regulation of Saccharomyces Rad53 checkpoint kinase during adaptation from DNA damage-induced G2/M arrest. *Mol Cell* **7**: 293–300.

Pierce AJ, Hu P, Han M, Ellis N, Jasin M. (2001). Ku DNA end-binding protein modulates homologous repair of double-strand breaks in mammalian cells. *Genes Dev* **15**: 3237–3242.

Rooney S, Sekiguchi J, Whitlow S, Eckersdorff M, Manis JP, Lee C *et al*. (2004). Artemis and p53 cooperate to suppress oncogenic N-myc amplification in progenitor B cells. *Proc Natl Acad Sci USA* **101**: 2410–2415.

Schmuckli-Maurer J, Rolfsmeier M, Nguyen H, Heyer WD. (2003). Genome instability in rad54 mutants of Saccharomyces cerevisiae. *Nucleic Acids Res* **31**: 1013–1023.

Smiraldo PG, Gruver AM, Osborn JC, Pittman DL. (2005). Extensive chromosomal instability in Rad51d-deficient mouse cells. *Cancer Res* **65**: 2089–2096.

Sung P. (1994). Catalysis of ATP-dependent homologous DNA pairing and strand exchange by yeast RAD51 protein. *Science* **265**: 1241–1243.

Taccioli GE, Amatucci AG, Beamish HJ, Gell D, Xiang XH, Torres Arzayus MI *et al*. (1998). Targeted disruption of the catalytic subunit of the DNA-PK gene in mice confers severe combined immunodeficiency and radiosensitivity. *Immunity* **9**: 355–366.

Tanori M, Mancuso M, Pasquali E, Leonardi S, Rebessi S, Di Majo V *et al*. (2008). PARP-1 cooperates with Ptc1 to suppress medulloblastoma and basal cell carcinoma. *Carcinogenesis* **29**: 1911–1919.

Tischfield JA, Shao C. (2003). Somatic recombination redux. *Nat Genet* **1**: 5–6.

Tong WM, Ohgaki H, Huang H, Granier C, Kleihues P, Wang ZQ. (2003). Null mutation of DNA strand break-binding molecule poly(ADP-ribose) polymerase causes medulloblastomas in p53(−/−) mice. *Am J Pathol* **162**: 343–352.

Tutt A, Gabriel A, Bertwistle D, Connor F, Paterson H, Peacock J *et al*. (1999). Absence of Brca2 causes genome instability by chromosome breakage and loss associated with centrosome amplification. *Curr Biol* **9**: 1107–1110.

Vogel H, Lim DS, Karsenty G, Finegold M, Hasty P. (1999). Deletion of Ku86 causes early onset of senescence in mice. *Proc Natl Acad Sci USA* **96**: 10770–10775.

Wang W, Seki M, Narita Y, Sonoda E, Takeda S, Yamada K *et al*. (2000). Possible association of BLM in decreasing DNA double strand breaks during DNA replication. *EMBO J* **19**: 3428–3435.

Weinstock DM, Jasin M. (2006). Alternative pathways for the repair of RAG-induced DNA breaks. *Mol Cell Biol* **26**: 131–139.

Xu X, Weaver Z, Linke SP, Li C, Gotay J, Wang XW *et al*. (1999). Centrosome amplification and a defective G2-M cell cycle checkpoint induce genetic instability in BRCA1 exon 11 isoform-deficient cells. *Mol Cell* **3**: 389–395.

Yan CT, Kaushal D, Murphy M, Zhang Y, Datta A, Chen C *et al*. (2006). XRCC4 suppresses medulloblastomas with recurrent translocations in p53-deficient mice. *Proc Natl Acad Sci USA* **103**: 7378–7383.

Yoshihara T, Ishida M, Kinomura A, Katsura M, Tsuruga T, Tashiro S *et al*. (2004). XRCC3 deficiency results in a defect in recombination and increased endoreduplication in human cells. *EMBO J* **23**: 670–680.